NIPPON STEEL & SUMITOMO METAL TECHNICAL REPORT No. 114 MARCH 2017

Technical Report

UDC 621 . 78 . 066 . 6 - 936 . 7

Measurement Technique of Solubility of Metal Oxides in Melts for Controlling the Solid-liquid Interface Reactions at High Temperatures

Ryutaro TOKI* Takashi DOI
Nobuo OTSUKA

Abstract

To control the solubility behavior of metal oxides in melts which is one of the solid-liquid interface reactions at high temperatures, this study is aimed at establishing the measurement technique of the solubility of metal oxides to binary $Na_2B_4O_7$-B_2O_3 melt focused on the basicity. The basicity sensor using the solid electrolytes was employed. The correlation between the basicity and the solubility of the metal oxides in the melt was revealed by the measurement technique. From the solubility dependence on the melt basicity, both the quantitative assessment of the solubility of the metal oxides and the estimate of the dissolution reactions of the metal oxides were allowed.

1. Introduction

Processes involved in steel products frequently cause the steel materials, refractories, and scales to contact melts (slag, antioxidants, etc.) under high temperatures. Various reactions occur at the solid-liquid interface formed when there is such contact at high temperatures. For example, reactions in the steelmaking process include the metal oxide dissolution reaction[1], which occurs at the interface between slag and an oxide refractory, and electrochemical reactions[2] via an antioxidant between molten steel and an immersion nozzle refractory. It is important to control the solid-liquid interface reactions at high temperatures, which are considered to precipitate the erosion of a refractory or nozzle clogging. However, since it is difficult to actually measure a reaction that is occurring at the solid-liquid interface under high temperatures, there are several issues to be resolved. To control the solid-liquid interface reactions occurring at high temperatures, it is important to identify the factors that control each phenomenon while clarifying it. Therefore, in this study, we establish measurement technology under a condition at high temperatures, which will be instrumental in clarifying the solid-liquid interface reactions at high temperatures.

One of the dominant factors of the solid-liquid interface reactions at high temperatures is O^{2-} activity. Similar to a solution system in which the H^+ activity represents pH, in molten oxide systems, the O^{2-} activity represents basicity.[3] Therefore, in order to explain the solid-liquid interface reactions at high temperatures, the basicity measurement technology such as a pH meter is thought to be useful. However, it is very difficult to actually measure the O^{2-} activity. Consequently, basicity that can be used as the indexes to be measured or calculated has been suggested. Such indexes include the basicity that is defined by the mass ratio of CaO/SiO_2 well-known in the field of slag[2], the optical basicity proposed by Duffy, et al.[4], and the basicity that is defined by Na_2O activity (a_{Na_2O})[2]. In this study, the use of basicity B that is defined by Na_2O activity shown in equation (1) is considered. The reason for this includes the fact that the set measurement of basicity B under high temperatures can be performed relatively easily using a basicity sensor[5–13] that uses a solid electrolyte.

$$B = -\log a_{Na_2O} \quad (1)$$

The solubility behavior of metal oxides in melts based on the basicity B described above has already been investigated, in which the fluxing model is known as the melting reaction mechanism. With this model, the basicity of a melt is acid (low Na_2O activity), and the dissolution reaction of a metal oxide accords with the basicity solubility; when the basicity of a melt is basic (high Na_2O activity), it accords with acid solubility.[5–7] To clarify the solubility behav-

* Researcher, Fundamental Metallurgy Research Lab., Advanced Technology Research Laboratories
1-8 Fuso-cho, Amagasaki, Hyogo Pref. 660-0891

ior of protective oxide films in melts of sulfuric acid considered to involve the abnormal corrosion of gas turbines used for airplanes/power generation, the metal oxide solubility of Fe_2O_3, Cr_2O_3, Al_2O_3, SiO_2, etc. depending on the basicity of Na_2SO_4 melts has been reported.[5–7] Since the measurement technology used for this molten Na_2SO_4 allows for estimation of the oxide solubility and the dissolution reaction formula, we examined the application of the fluxing model to the molten metal oxide system used in the processes involved in steel products.

The binary Na_2O-B_2O_3 melt has long been used for various fields related to the surface cleaner[14] to remove oxides on metal surfaces, boronizing of steel surfaces[15] using salt baths, and slag components, etc. For the melt systems, whereas the basicity measurement[3, 12, 13] has been reported, the detailed influence of the basicity on the metal oxide solubility has yet to be elucidated.

Therefore, this study investigates a Na_2O-B_2O_3 melt, which melts at low temperature and is easily handled, with the aim of establishing the measurement technology of metal oxide solubility for the basicity in order to clarify the metal oxide dissolution reactions.

2. Experiment Method[16]

2.1 Basicity sensor

In this study, the application of the basicity sensor[5–7] used for the measurement of the basicity of a Na_2SO_4 melt to a $Na_2B_4O_7$-B_2O_3 melt was examined. **Figure 1** shows a schematic view of the basicity sensor prepared. The basicity sensor consists of two sensors: an oxide ion sensor and oxygen sensor. Each sensor is described below.

2.1.1 Oxide ion sensor

Within an oxide ion sensor, mullite[5–7], β-alumina[3, 12, 13], or quartz glass[17, 18] is mainly used as a sodium ion solid electrolyte under high temperatures. In this study, the sensor was prepared using quartz glass, which is difficult to dissolve in a $Na_2B_4O_7$-B_2O_3 melt. As shown in Fig. 1, the electrochemical equilibrium reactions at electrode [A] and electrode [B] in the following cell, in which a quartz glass bulkhead is placed between electrode [A] and electrode [B],

$$(-)\,\mathrm{Ag}\,|\,\mathrm{Na_2SO_4\text{-}10\,mol\%Ag_2SO_4}\,||\,\mathrm{Na_2B_4O_7\text{-}B_2O_3}\,|\,\mathrm{Pt}\,(+),\ \mathrm{Air}$$

Electrode [A] | Quartz ← Na^+ → | Electrode [B]

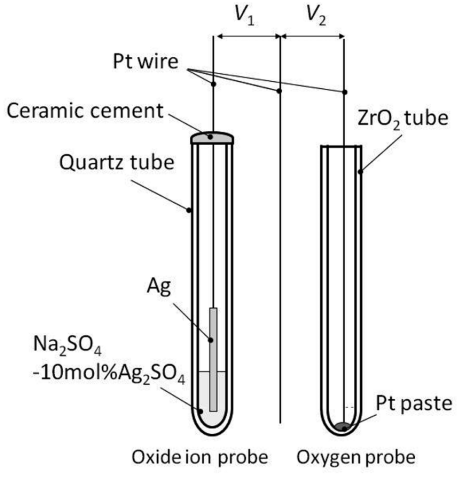

Fig. 1 Schematic representation of the basicity sensor

are indicated as follows.

$$\text{Electrode [A]}\quad Ag^+ + e^- = Ag \tag{2}$$

$$\text{Electrode [B]}\quad \frac{1}{2}O_2 + 2e^- = O^{2-} \tag{3}$$

The reaction at each electrode is indicated as

$$\text{Electrode [A]}\quad Ag_2SO_4 + 2e^- = 2Ag + SO_4^{2-} \tag{4}$$

$$\text{Electrode [B]}\quad 2Na^+ + \frac{1}{2}O_2 + 2e^- = Na_2O \tag{5}$$

and thereby equation (6) for the overall cell reaction can be obtained.

$$Na_2SO_4 + 2Ag + \frac{1}{2}O_2 = Na_2O + Ag_2SO_4 \tag{6}$$

Assuming that Na_2SO_4, Ag_2SO_4, and Na_2O are components 1, 2 and 3, the Gibbs free energy change of equation (6), ΔG, is written as

$$\Delta G = [\Delta G_3^O + \Delta G_2^O - \Delta G_1^O - RT\ln(a_1/a_2)] + RT\ln(a_3/P_{O_2}[B]^{1/2}) \tag{7}$$

Where R is the gas constant, T is the absolute temperature, a_i is the activity of the i component, ΔG_i^O is Gibbs standard free energy of the i component, and $P_{O_2}[B]$ is the oxygen potential on the side of electrode [B].

When assuming regular solution approximation $a_i = \gamma_i N_i$ (γ_i: i component activity factor, N_i: i component molar fraction), a_1/a_2 is indicated as

$$\begin{aligned} a_1/a_2 &= \gamma_1 N_1/\gamma_2 N_2 \\ &= (N_1/N_2)(\gamma_1/\gamma_2) \\ &= (N_1/N_2)\exp[\alpha(N_2^2 - N_1^2)/(RT)] \end{aligned} \tag{8}$$

$$\gamma_1/\gamma_2 = \exp[\alpha(N_2^2 - N_1^2)/(RT)] \tag{9}$$

Then the ratio of γ_1/γ_2 is indicated as equation (9) using the interaction constant α of a Na_2SO_4-Ag_2SO_4 mixed melt at temperature T.[17]

Equation (8) is substituted into equation (7) using the value of Gibbs standard free energy for Na_2SO_4, Ag_2SO_4 and Na_2O at 1 173 K[19], and electromotive force V_1 is obtained from equation (10),

$$V_1 = -\Delta G/(2F) = -1.448 - 0.116\log\left[\frac{a_{Na_2O}}{(P_{O_2}[B])^{1/2}}\right] (at\ 1173\,K,\ V_1\ in\ V) \tag{10}$$

where F represents the Faraday constant. Here, a_{Na_2O} can be obtained from $P_{O_2}[B]$ measured using the oxygen probe described later and electromotive force V_1.

2.1.2 Oxygen sensor

Stabilized zirconia (Y_2O_3-ZrO_2, MgO-ZrO_2, CaO-ZrO_2, etc.), which is an oxide ion solid electrolyte has often been employed as an oxygen sensor. As shown in Fig. 1, after fixing the platinum wire with platinum paste to the internal surface at the bottom of the stabilized zirconia tube (Y_2O_3-ZrO_2), the tube was heated thereby adhering the platinum wire.

Electromotive force V_2 between the electrodes of the following cell, in which a zirconia bulkhead is placed between electrode [A] and electrode [B],

$$(-)\,\mathrm{Pt}\,|\,\mathrm{air}\,(P_{O_2} = 0.21\,\mathrm{atm})\,||\,\mathrm{Na_2B_4O_7\text{-}B_2O_3}\,|\,\mathrm{Pt}\,(+)$$

Electrode [A] | ZrO_2 ← O^{2-} → | Electrode [B]

depends on the oxygen potential on both sides of the zirconia bulkhead. When dried air is used as the standard gas on the electrode [A] side, $P_{O_2}[B]$ can be obtained from equation (11).

$$V_2 = \frac{RT}{4F}\ln\left(\frac{0.21}{P_{O_2}[B]}\right) \tag{11}$$

2.2 Basicity measurement of $Na_2B_4O_7$-B_2O_3 melt

Using the basicity sensor prepared, the basicity of the $Na_2B_4O_7$-B_2O_3 melt was measured in air at 1 173 K. **Figure 2** shows a schematic view of the experimental setup and **Table 1** shows the composition of the sample melt used for the measurement. From the Na_2O-B_2O_3 phase diagram[20], it was confirmed that the Na_2O-B_2O_3 melt in the composition range used in this study would completely melt at 1 173 K. Powdery $Na_2B_4O_7$ and B_2O_3 were mixed, melted in a platinum crucible at 1 173 K in air and it was maintained for 25.2 ks or more. The basicity sensor was immersed in the melt to a depth of 5 mm under the liquid surface and each electromotive force V_1 and V_2 of the basicity sensor was measured. Both V_2 and V_2 were measured by a potentiostat and were recorded by a data logger.

2.3 Dissolution behavior change of metal oxides in the $Na_2B_4O_7$-B_2O_3 melt

In order to measure the solubility of the metal oxide, the testing equipment shown in Fig. 2 was used. **Table 2** shows the composition of the melt used for the measurement. The powdery metal oxides (Fe_2O_3 and Cr_2O_3), the quantity of which was examined and confirmed to be more than the saturation solubility, was put in advance at the bottom of the platinum crucible. To secure the chemical equilibrium of the molten $Na_2B_4O_7$-B_2O_3 including the Fe_2O_3 or Cr_2O_3, the melts were heated at 1 173 K for 86.4 ks or more in air. After heating it, the basicity of the melt was measured using the basicity sensor. Then, the sample for analysis was taken immediately using a platinum wire with the tip coiled. The component concentration of the sample was analyzed using a high-frequency inductively coupled plasma atomic emission spectroscopy (ICP-AES), and Fe and Cr in the melt were quantitatively determined. Each mass of Fe_2O_3 and Cr_2O_3 dissolved in the sample was calculated from the quantitative values acquired and the solubility was obtained. This was based on the assumption of the metal ion that was uniformly distributed in the melt.

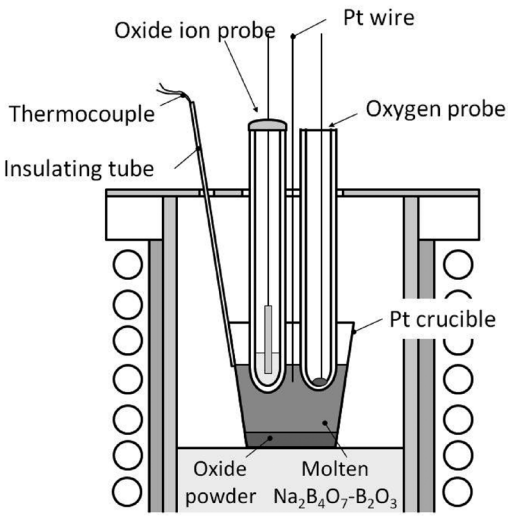

Fig. 2 Experimental setup of melt basicity and oxide solubility measurements in $Na_2B_4O_7$-B_2O_3 melt

Table 1 Salt compositions used for the basicity measurement

Sample No.	$Na_2B_4O_7$	B_2O_3
1	100	0
2	80	20
3	50	50
4	30	70
5	10	90

(in mass%)

Table 2 Salt compositions used for the oxide solubility measurement

Sample No.	$Na_2B_4O_7$	B_2O_3
1	100	0
2	90	10
3	80	20
4	70	30
5	60	40
6	50	50

(in mass%)

3. Results[16]

3.1 Basicity measurement of the $Na_2B_4O_7$-B_2O_3 melt

Figure 3 shows the $Na_2B_4O_7$-B_2O_3 melt measurement values at 1 173 K in air together with the values obtained by Itoh, et al.[12] for comparison. The horizontal axis of Fig. 3 represents the molar fraction $X_{B_2O_3}$ of B_2O_3, and the vertical axis represents the basicity. From Fig. 3, the basicity of the melt was changed to acid along with the increase in the B_2O_3 rate. The values measured by Itoh, et al.[12] using a different method from this study accorded with those in this study well, and almost the same measurement results were obtained.

3.2 Measurement of the solubility of metal oxides in the $Na_2B_4O_7$-B_2O_3 melt

Figure 4 shows the measurement results of the solubility of the metal oxides as a function of the basicity of the $Na_2B_4O_7$-B_2O_3 melt. The horizontal axis of Fig. 4 represents the basicity and the vertical axis the common logarithms of solubility W. In the basicity range measured, the solubility of Fe_2O_3 was larger than that of Cr_2O_3, indicating a tendency in which the solubility of both metal oxides declined when the basicity showed acidity.

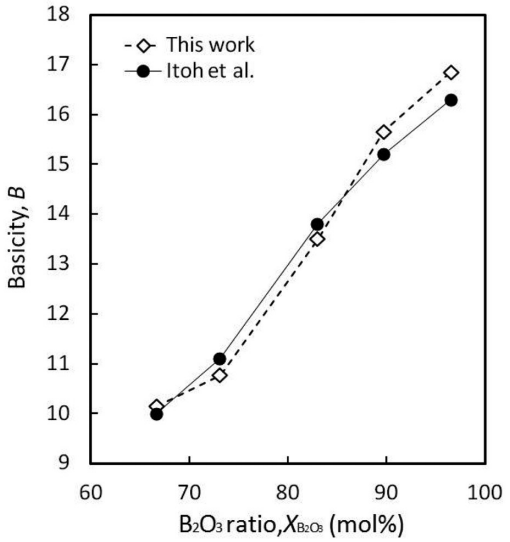

Fig. 3 Measured basicity of the $Na_2B_4O_7$-B_2O_3 melt as a function of B_2O_3 ratio of the melt at 1173K in air
Literature[12] data were superimposed.

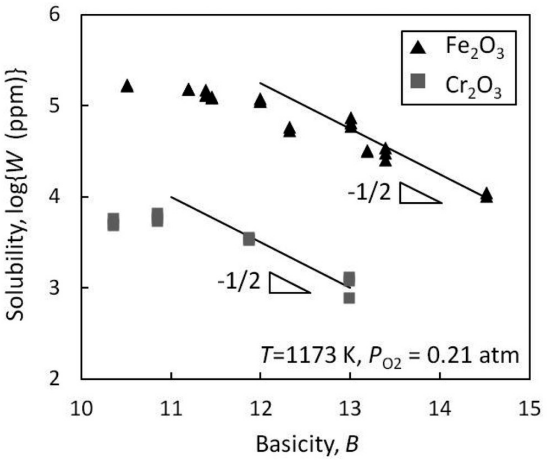

Fig. 4 Common logarithm of M_2O_3 concentration (M=Fe, Cr) in mass in fused $Na_2B_4O_7$-B_2O_3 at 1 173 K in air as a function of basicity of the $Na_2B_4O_7$-B_2O_3 melt

4. Discussion[16)]

4.1 Measurement of the basicity of the $Na_2B_4O_7$-B_2O_3 melt

It is inferred that the dissociation equilibrium reaction expressed by equation (12) and equation (13) occurs in the molten $Na_2B_4O_7$-B_2O_3. The cause of the increase of the B_2O_3 rate prompting the basicity change to acid was considered to be the decline of the O^{2-} activity (Na_2O activity) in the melt due to the reaction of B_2O_3 expressed by equation (13). Since the measurement results of this study accorded well with the results by Itoh, et al.,[12)] we determined that the measurement method of this study can be used for the measurement of the basicity of Na_2O-B_2O_3 melts at 1 173 K in air.

$$Na_2O = 2Na^+ + O^{2-} \quad (12)$$

$$B_2O_3 + O^{2-} = 2BO_2^- \quad (13)$$

4.2 Dependence of the solubility of metal oxides on the basicity

Since the solubility of Fe_2O_3 and Cr_2O_3 declined along with the change of the basicity of the melt to acid, it was considered that both metal oxides were dissolved as a result of the basic dissolution reactions in the basicity measurement range of this study. Each basic dissolution reaction of Fe_2O_3 and Cr_2O_3 was estimated as follows.[5)]

$$Fe_2O_3 + Na_2O \rightarrow 2NaFeO_2 \quad (14)$$

$$Cr_2O_3 + Na_2O \rightarrow 2NaCrO_2 \quad (15)$$

Equilibrium constants K_1 and K_2 in equations (14) and (15) are expressed as follows.

$$K_1 = \frac{(a_{NaFeO_2})^2}{a_{Fe_2O_3} \cdot a_{Na_2O}} \quad (16)$$

$$K_2 = \frac{(a_{NaCrO_2})^2}{a_{Cr_2O_3} \cdot a_{Na_2O}} \quad (17)$$

When the common logarithms of both sides in equation (16) and equation (17) are used and the formula is changed, the following equations are obtained.

$$\log a_{NaFeO_2} = -\frac{1}{2}(-\log a_{Na_2O} + C_1),\ C_1 = -\log K_1 - \log a_{Fe_2O_3} \quad (18)$$

$$\log a_{NaCrO_2} = -\frac{1}{2}(-\log a_{Na_2O} + C_2),\ C_2 = -\log K_2 - \log a_{Cr_2O_3} \quad (19)$$

When both sides in equation (18) and equation (19) are partially differentiated by $-\log a_{Na_2O}$,

$$\left(\frac{\partial \log a_{NaFeO_2}}{\partial(-\log a_{Na_2O})}\right) = \left(\frac{\partial \log a_{NaCrO_2}}{\partial(-\log a_{Na_2O})}\right) = -\frac{1}{2} \quad (20)$$

The equation (20) expresses the inclination of the common logarithms of solute concentration in the melt for the basicity. In other words, when the inclination of the straight line in Fig. 4 aligns with equation (20), it is considered that both metal oxides are dissolved according to reaction equations (14) and (15).[5, 7)] In Fig. 4, when the basicity of the melt was in the range between 12 and 14.5, the straight line inclination obtained from the measurement was −1/2, aligning with equation (21). From this, we determined that the dissolution reactions of Fe_2O_3 and Cr_2O_3 conformed to the basic dissolution in equation (14) and equation (15).

In the Na_2O-B_2O_3 melt, the measurement results in this study showed that the solubility of Cr_2O_3 was smaller than that of Fe_2O_3. From this, it is estimated that the metal oxide solubility causes the difference between pure Fe and pure Cr in the formation of a protective oxide film, exerting influence on the corrosion behavior in each metal. In other words, if the oxide solubility measurement results obtained in this study are reasonable, then it is estimated that as the solubility of Fe_2O_3 increases, the Na_2O-B_2O_3 melt will corrode pure Fe more than pure Cr. To evaluate the validity of the metal oxide solubility measurement results in this study in view of the hot corrosion behavior of metals, an immersion test was performed using test piece plates of pure Fe and pure Cr in a $Na_2B_4O_7$ melt at 1 173 K under the condition of the open atmosphere.

Figure 5 shows the appearance of Fe and Cr test pieces after the immersion test. After the immersion, the pure Fe was locally and intensely dissolved in the part of the gas-liquid interface of the melt in 0.3 ks. In 0.6 ks after the immersion, the pure Fe plate was broken at the gas-liquid interface of the melt. On the other hand, the pure Cr plate, unlike the pure Fe, did not dissolve or break at the gas-liquid interface.

It is estimated that the state described above was caused as the metal oxide formed on the metal surface due to hot corrosion was dissolved to the melt, no protective film was formed and the corrosion was unable to be suppressed. As previously estimated, since the solubility of the iron oxide in the $Na_2B_4O_7$ melt is sufficiently large, the Fe test piece was locally and intensely dissolved. In contrast, it is considered that since the solubility of the chromium oxide was smaller than that of the iron oxide, the protective film was easily formed on the Cr test piece compared to the Fe, because of which it was not much dissolved. Moreover, it is considered that in the local dissolution of the pure Fe test piece, the Marangoni effect prevailed, similar to the local erosion of an oxide refractory by a melt.[2)] From these, we concluded that the relationships involved in the increase/decrease of the solubility of Fe_2O_3 and Cr_2O_3 to the Na_2O-B_2O_3 melt

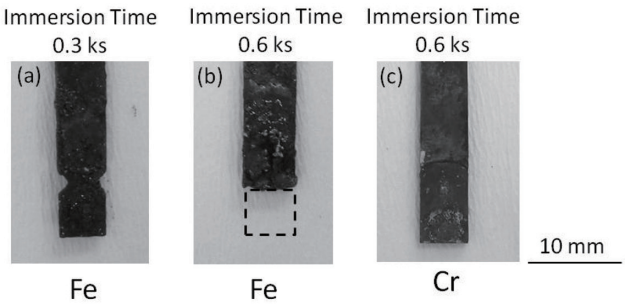

Fig. 5 Specimen appearance after immersion in the fused $Na_2B_4O_7$ melt at 1 173 K in air
(a) Pure Fe specimen (immersion time: 0.3 ks)
(b) Pure Fe specimen (immersion time: 0.6 ks)
(c) Pure Cr specimen (immersion time: 0.6 ks)

derived from the measurement results in this study were reasonable.

5. Conclusion

The technique for measuring the solubility of metal oxides to a $Na_2B_4O_7$-B_2O_3 melt using a basicity sensor was established. The application of the fluxing model allowed for estimation of the solubility of metal oxides to basicity as well as the oxide dissolution reaction equations. Details of the results of this study are as follows.

(1) The sensor used for the basicity measurement of a Na_2SO_4 melt was employed for the basicity measurement of a $Na_2B_4O_7$-B_2O_3 melt, and the measurement of the basicity under the conditions at 1 173 K and of the open atmosphere was allowed.

(2) When the basicity of the $Na_2B_4O_7$-B_2O_3 melt was in the range from 10 to 13, the solubility of Fe_2O_3 was one order of magnitude higher than that of Cr_2O_3.

(3) In the basicity range from 12 to 14.5, the solubility of both Fe_2O_3 and Cr_2O_3 decreased with the increase of the basicity of the melt. It was concluded that the dissolution reactions of both metal oxides followed the basic dissolution in the fluxing model applied.

The basicity measurement was useful in the set measurement to understand the dissolution behavior of metal oxides in a melt.

References

1) Mukai, K.: Interface Physical Chemistry of High Temperature Melts. 1st Edition. Tokyo, AGNE Gijutsu Center, 2007
2) Tsukaguchi, Y. et al.: Materia Japan. 50 (1), 27 (2011)
3) Yokokawa, T.: Chemistry of High Temperature Melts. 1st Edition. Tokyo, AGNE Gijutsu Center, 1998
4) Duffy, J. A. et al.: J. Non-Crysta. Solids. 21, 373 (1976)
5) Rapp, R. A. et al.: JOM. December, 47 (1994)
6) Fukumoto, M. et al.: Journal of the Society of Materials Engineering for Resources of Japan. 15 (1), 16 (2002)
7) Otsuka, N.: Corrosion Engineering. 38, 608 (1989)
8) Yamaguchi, S. et al.: J. Japan Inst. Met. Mater. 47 (9), 736 (1983)
9) Tsukihashi, F. et al.: Tetsu-to-Hagané. 71 (7), 815 (1985)
10) Abdelouhab, S. et al.: J. Non-Crystalline Solids. 354, 3001 (2008)
11) Kim, W. S. et al.: Thermochimica Acta. 414, 191 (2004)
12) Itoh, H. et al.: J. Chem. Soc. Faraday Trans. 1. 80, 473 (1984)
13) Yokokawa, T.: Materia Japan. 34 (1), 65 (1995)
14) Rus, J. et al.: J. Mater. Sci. Lett. 4, 558 (1985)
15) Wang, J. et al.: J. Wuhan Univ. Technology Mater. Sci. Ed. 26, 1137 (2011)
16) Toki, R. et al.: J. Japan Inst. Met. Mater. 78 (10), 395 (2014)
17) Shores, D. A. et al.: J. Appl. Electrochem. 10, 275 (1980)
18) Mittal, S. et al.: J. Electrochem. Soc. 134, 244 (1987)
19) Chase, M. W. et al.: JANAF Thermochemical Tables. 3rd Ed. American Chemical Society, 1986
20) Levin, E. M. et al.: Phase Diagrams for Ceramists 1975 Supplement. 1st Ed. Ohio, The American Ceramic Society, 1975

Ryutaro TOKI
Researcher
Fundamental Metallurgy Research Lab.
Advanced Technology Research Laboratories
1-8 Fuso-cho, Amagasaki, Hyogo Pref. 660-0891

Takashi DOI
Senior Researcher, Dr. Eng
Fundamental Metallurgy Research Lab.
Advanced Technology Research Laboratories

Nobuo OTSUKA
Dr. Eng
Amagasaki Division
Nippon Steel & Sumikin Technology Co., Ltd.